# Off-center electron transport in resonant tunneling diodes due to incoherent scattering

Titus Sandu,[1,*] Gerhard Klimeck,[2,†] and W. P. Kirk[1]
[1]*NanoFAB Center, Electrical Engineering Department, University of Texas at Arlington, Arlington, Texas 76019, USA*
[2]*Jet Propulsion Laboratory, California Institute of Technology, Pasadena, California 91109, USA*
(Received 25 March 2003; published 26 September 2003)

Coherent transport through resonant tunneling diodes at high bias is determined by the transfer of carriers described by momentum and energy from a bath in the emitter through a central resonance to the collector. Simplified treatments of coherent carrier transport assume the transverse carrier dispersions to be identical and parabolic in the emitter and central device. This results in a carrier transport that is dominated by carriers at the $\Gamma$ zone center. Other work has shown that more realistic dispersions result in off-zone center current flow. Incoherent scattering adds more degrees of freedom to match the emitter energy and momentum $(E_{em},k_{em})$ with the resonance energy and momentum $(E_{res},k_{res})$ with $(\Delta E_{scatt},\Delta k_{scatt})$. It is shown analytically and numerically that this additional degree of freedom redirects carriers in energy and momentum space resulting in an off-zone center current for large voltage regions. Interface roughness, polar optical phonon, and acoustic phonon scatterings are explicitly considered.

DOI: 10.1103/PhysRevB.68.115320 PACS number(s): 73.40.Gk, 72.80.Ey, 71.20.−b, 73.20.At

## I. INTRODUCTION

Multilayered heterostructures are realized by the deposition of different semiconductors with an atomic accuracy of the interfaces. The incorporated potential due to band offsets of the constituent materials is used to build wells and barriers for devices such as resonant tunneling diodes (RTDs), quantum well infrared detectors, quantum well lasers, and heterostructure field effect transistors. RTDs are interesting electronic devices due to their N-shaped current-voltage characteristics, which can be utilized for memory cells[1] and ultrafast analog digital converters.[2] The basic mechanism of the current turn-on and turn-off in a RTD is the crossing of the central resonance subband with the Fermi level in the emitter and the ''effective'' band edge in the emitter. The ''effective'' emitter band edge may be the bulk three dimensional (3D) band edge in a flat band emitter or the bottom of the subband of quasi-bound emitter states.

The carrier transport through a RTD can be viewed as the voltage dependent movement of an energy and momentum dependent band-pass filter through an energy and momentum dependent electron supply function. The band-pass filter is dominated in its characteristics by the central resonance state. The electron supply function is determined at the low energy end by the bottom of the conduction band and at the high energy end by the Fermi level. Current turns on as the resonance is pulled from high energies into the Fermi-sea and turns off as the resonance is pulled past the bottom of the emitter conduction band. The 1D heterostructure quantizes the carrier degrees of freedom in the growth direction described by a quantized energy $(E_z)$. The two transverse directions are typically assumed to be of infinite extent and plane waves are used as a basis set described by a particular energy $(E_{trans})$ and momentum $(k)$ relation. The total energy $(E_t)$ of the carrier has therefore two contributions $(E_t=E_z+E_{trans})$.

Carriers can be transmitted through the central resonance described by $E_z$ and $k$, if a carrier with that quantized energy and transverse momentum can be supplied in the emitter. This description corresponds numerically to a double integral over $E_z$ and $k$ of a $E_z$ and $k$ dependent transfer function. The double integral is numerically intensive to perform, due to the very strong variations in the integrand. This can be attributed to the long coherent resonance state lifetimes in typical systems which result in typical energy linewidths that are typically in the range of a few $\mu$eV which need to be resolved well in an energy range of typically 0.5 eV.[3]

In the simplest and most discussed case of electron transport in RTDs the transverse dispersions are considered to be parabolic, and the integral over transverse momenta can be performed analytically since all transverse momenta in the emitter match those in the central resonance. A single integral over energy is left to be performed numerically (Tsu-Esaki approximation).[4] Analytical results can be given in that case that the transport is dominated by zero transverse momentum carriers $(k=0)$.[5] If the transverse dispersions are treated more realistically for nonparabolic electron systems[6–9] and hole systems,[10,11] the Tsu-Esaki approximation has been proven to produce qualitatively and quantitatively wrong results. Furthermore it has been shown that conditions exist in large voltage ranges of operation where nonzero transverse momentum carriers dominate the transport. Off-center current flow implies that significantly more carriers move through the structure at an angle than straight through. Three mechanisms were identified as the origin of the off-center flow:[5,11] nonmonotonic dispersion, resonance linewidth modulation, and a lighter well than emitter effective mass. All three mechanisms are present in hole systems, where the off-center current flow has been recently proven experimentally.[12] The third mechanism has been proven numerically in Ref. 13 and can be described with a modified Tsu-Esaki formula to account for different emitter and well in-plane masses.[14]

Such an off-center current flow is induced by the detailed selection energy and momentum of the coherently transmitted carriers. This work explores another source of off-center carrier transport. Carriers in the emitter reservoirs need to match the quantized energy $E_z$ and transverse momentum $k$ of the available resonance state in the central device region.

 

Given a total energy $E_t$ and transverse momentum $k$ in the emitter, a scattering event can provide the required $\Delta E$ or $\Delta k$ to match the central resonance requirement. After the scattering event, the carrier travels through the structure with $E_z = E_{resonance}$ and $k_{modified}$. In the case of elastic scattering, the physical effect is a redirection of the electron momentum without a loss of the total energy. Energy is only ''lost'' in the forward traveling direction. Such a loss of energy has also been termed ''vertical flow,''[15] where vertical refers to the energy scale in an energy resolved analysis of electron flow in quantum devices. The case of inelastic scattering is a bit more complicated since the total energy of the scattered carrier changes. Such scattering events couple different total energies as discussed in more detail in Ref. 16. The effect of the redistribution of carriers in energy and momentum space is the subject of this paper. We shall show this numerically using the nanoelectronic modeling (NEMO) program. The whole treatment assumes a single band effective mass model with spatially varying effective masses. The numerical approach is based on nonequilibrium Green function formalism, which includes scattering effects through self-energy terms in a single band model. The theory is documented in Ref. 16.

The paper is organized as follows. In the Sec. II we present the analytical argument that leads to the off-center current flow. The numerical results are discussed in Sec. III.

## II. ANALYTICAL RESULT

The form for the total Hamiltonian is

$$H = H_0 + H_S. \tag{1}$$

$H_0$ describes the unperturbed system, and $H_S$ accounts for all the scattering terms. In terms of creation and annihilation operators, $H_0$ can be written as the standard tunneling Hamiltonian:

$$H_0 = \sum_{k,\sigma,\alpha\in L,R} \varepsilon_{k\alpha} a^+_{k\sigma\alpha} a_{k\sigma\alpha} + \sum_{k,\sigma} \varepsilon^w_k b^+_{k\sigma} b_{k\sigma} + \sum_{k,\sigma,\alpha\in L,R} (V_\alpha a^+_{k\sigma\alpha} b_{k\sigma} + \text{H.c.}). \tag{2}$$

Here $a^+_{k\sigma\alpha}(a_{k\sigma\alpha})$ creates (annihilates) an electron with transverse momentum $k=(k_x,k_y)$ and spin $\sigma$ in channel $\alpha$ in either the left ($L$) or the right ($R$) contact and $b^+_{k\sigma}(b_{k\sigma})$ is the creation (annihilation) operator in the well with transverse momentum $k$ and spin $\sigma$. The channel index includes all other quantum numbers to define, in addition to $k$ and $\sigma$, a state in the contacts. $V_\alpha$ are the hopping matrix elements between contacts (emitter and collector) and the central well and can be calculated according to Bardeen prescription[17] or tight binding.[18] They depend on the barrier profiles and include the effect of applied potential. $\varepsilon^w_k = \varepsilon_0 + \beta eV + \mathbf{k}^2/2m^*_W$ is the resonance level affected by the bias voltage ($\beta$ is the structure dependent factor and is about 0.5 for symmetric wells and $\boldsymbol{k}$ is the in-plane momentum). The energy in the emitter is $\varepsilon_{k\sigma\alpha} = \mathbf{k}^2/2m^*_E + E_\alpha$ with $\boldsymbol{k}$ is the transverse momentum and $E_\alpha$ is either $k^2_{//}/2m^*_E$ for 3D states (scattering states) in the emitter or $E_\alpha = E_{no}$, the energy levels for 2D quasibound states in the emitter notch. The collector states (right contact) have the energy $\varepsilon_{k\sigma\alpha} = (\mathbf{k}^2 + k^2_{//})/2m^* - eV$, with $V$ the applied bias voltage.

Using the nonequilibrium Green function formalism one can show that the formula for the current that flows from the left contact to the central region is as follows:[16,19]

$$J_L = \frac{e}{\hbar}\int \frac{d\omega}{2\pi} \sum_{k,\sigma,\alpha\in L} |V_\alpha|^2 [A_{k\sigma}(\omega) f_L(\omega) + iG^<_{k\sigma}(\omega)] a_{k\sigma\alpha}(\omega), \tag{3}$$

where $a_{k\sigma\alpha}(\omega)$ is the spectral function of the emitter, and $A_{k\sigma}(\omega)$ and $G^<_{k\sigma}(\omega)$ are the spectral function and correlation function of the well, respectively. A similar equation can be expressed for the collector side of the system reflecting the current conservation across the active region. In a detailed form, the current density can be written as follows:

$$J_L = \frac{e}{\hbar}\int \frac{d\omega}{2\pi} \sum_{k,\sigma,\alpha\in L} |V_\alpha|^2 a_{k\sigma\alpha}(\omega) \times \frac{\Gamma^{T_R}_{k\sigma}(\omega)(f_L(\omega) - f_R(\omega)) + 2\Gamma^{Scatt}_{k\sigma}(\omega) f_L(\omega) + i\Sigma^{<,Scatt}_{k\sigma}}{[\omega - \varepsilon^w_{k\sigma} - \Lambda^T_{k\sigma}(\omega) - Re(\Sigma^{R,Scatt}_{k\sigma}(\omega))]^2 + \left(\frac{\Gamma^T_{k\sigma}(\omega)}{2} + Im(\Sigma^{A,Scatt}_{k\sigma}(\omega))\right)^2}. \tag{4}$$

Here $\Sigma^{<,Scatt}_{k\sigma}(\omega)$, $\Sigma^{R,Scatt}_{k\sigma}(\omega)$, and $\Sigma^{A,Scatt}_{k\sigma}(\omega)$ are the scattering self-energies; $\Gamma^{Scatt}_{k\sigma}$ is the imaginary part of $\Sigma^{R,Scatt}_{k\sigma}(\omega)$; $\Gamma^T_{k\sigma}$ and $\Lambda^T_{k\sigma}$ are imaginary and real part of tunneling self-energy, respectively; $\Gamma^L$ is the partial level width function; $\Gamma^{T_R}_{k,\sigma}$ the right-hand partial level width due to tunneling; and $f_L(\omega)$ and $f_R(\omega)$ are the Fermi functions in the left- and right-hand leads, respectively. The scattering self-energies $\Sigma^{<,Scatt}_{k\sigma}(\omega)$, $\Sigma^{R,Scatt}_{k\sigma}(\omega)$, and $\Sigma^{A,Scatt}_{k\sigma}(\omega)$ include any other interactions like the electron-electron interaction, electron-phonon interaction, interface roughness, etc., and, in principle, can be considered by using nonequilibrium perturbation theory.

We now define the framework for the Tsu-Esaki formula.[4] In that framework the transport is coherent and we neglect the scattering assisted tunneling. In this spirit we set to zero $\Sigma_{k\sigma}^{<,Scatt}(\omega)$, $\Sigma_{k\sigma}^{R,Scatt}(\omega)$, and $\Sigma_{k\sigma}^{A,Scatt}(\omega)$. Moreover the energy shift of quantum well state and its width due to tunneling are assumed constant. With these assumptions and the redefining of the integrand as $\omega \rightarrow \omega + k_{\perp}^2/2m_W^*$, we recover the classic Tsu-Esaki formula in one dimension.[4] In fact this redefinition makes the change from total energy parametrization to $E_z$, the energy along growth direction.

To include incoherent scattering, phenomenological Breit-Wigner form of transmission coefficient has been used.[20] Any energy modulation $\Lambda_{k\sigma}^T = \Lambda_{k\sigma}^T(\omega)$ and $\Gamma_{k\sigma}^T = \Gamma_{k\sigma}^T(\omega)$ as well as any energy modulation induced by scattering will break down the Tsu-Esaki formula and will induce an off-center current flow. To show the last assertion we make some approximations. We work in the wide-band limit, in which the bandwidth in the contacts is much larger than the resonance width, by assuming that the hopping matrix elements are nearly constant. We are interested in the peak and valley current; thus we can set $f_R(\omega)=0$. For the sake of simplicity we assume zero temperature and we set $\Sigma_{k\sigma}^{<,Scatt}(\omega)$ and the imaginary part of $\Sigma_{k\sigma}^{R,Scatt}(\omega)$ as constants and we focus on real part of $\Sigma_{k\sigma}^{R,Scatt}(\omega)$. The expansion of the real part of $\Sigma_{k\sigma}^{R,Scatt}(\omega)$ in series of $\boldsymbol{k}$, the transverse momentum, takes the form $Re(\Sigma_{k\sigma}^{R,Scatt}) = A + B\cdot\mathbf{k}^2$, where $A$ and $B$ are real constants. The constant $A$ acts like a renormalization of the well energy along the $z$ axis while $B$ renormalizes the effective mass. As we will see in Sec. III, $A$ is negative. If $B$ is positive, it means that the renormalized mass is smaller than emitter mass and we may expect off-zone center current flow.[13] In fact, from Eq. (4) one can get

$$J(k) \propto \int_0^{E_F - E_\perp} \frac{dE}{(E - \tilde{E}_z - B\cdot k^2)^2 + \Gamma^2}, \tag{5}$$

with $J_L = \Sigma_k J(k)$. In Eq. (5) $\Gamma = [\Gamma_{k\sigma}^T(\omega)/2] + \mathrm{Im}[\Sigma_{k\sigma}^{A,scatt}(\omega)]$ of Eq. (4), $\tilde{E}_z$ is the renormalized energy in the well along the $z$ axis, $E_F$ is the Fermi energy, and $E_\perp$ is the transverse energy. Changing the energy integration from total energy to longitudinal energy and dropping the dependence of the transverse direction $\phi$ enable integration over $E$:

$$J(k) \propto \Gamma \left( \arctan \frac{\tilde{E}_z + B\cdot k^2}{\Gamma} - \arctan \frac{\tilde{E}_z + E_\perp + B\cdot k^2 - E_F}{\Gamma} \right). \tag{6}$$

Equation (6), however, is a slight modification of Eq. (10) in Ref. 5. Here scattering is present by the additional $B$ term. Reference 4 uses the negative monotony of $J(k)$ to prove the generality of the zone center current flow in no-scattering, single-band, same effective mass transport. With $\lim_{k\rightarrow\infty} J(k) \rightarrow 0$ one can prove that $J(k)$ has a maximum at $k>0$ if $dJ(k)/dk > 0$. Having $E_\perp = \hbar^2 k^2/2m^*$, the derivative takes the form

$$\frac{dJ(k)}{dk} \propto \frac{Bk}{1 + \left( \dfrac{Bk^2 + \tilde{E}_z}{\Gamma} \right)^2} - \frac{Bk + \hbar^2 k/2m^*}{1 + \dfrac{[(\hbar^2/2m^* + B)k^2 + E_F - \tilde{E}_z]^2}{\Gamma^2}}. \tag{7}$$

In the vicinity of $k=0$ and $\tilde{E}_z$ approaching 0 (i.e., at current peak), a ratio $E_F/\Gamma > 10$ (which is one of the requirements of the wide-band approximation) and $B > 0.01(\hbar^2/2m^*)$ (perfectly reasonable) guarantee

$$\frac{dJ(k)}{dk} > 0 \tag{8}$$

and a maximum of $J(k)$ for $k \neq 0$, i.e. off-center current flow. Thus, one may expect that the mechanism of mass renormalization due to scattering could play a role in off-center current flow in resonant tunneling diodes. However, the mass renormalization induced by polar optical phonon scattering is positive[21] and, therefore, polar optical phonon scattering cannot contribute to the off-zone center current flow of electrons by this mechanism. The modulation of the linewidth can be treated in similar manner. In Sec. III we will show numerically that scattering induces off-center current flow in resonant tunneling diodes.

## III. NUMERICAL CALCULATIONS AND DISCUSSIONS

The test structure contains a 59.5-Å GaAs quantum well and 28.3-Å AlAs barriers. The double barrier structure is clad with undoped spacers of 195.5-Å thickness and high doping ($1\times10^{18}$ cm$^{-3}$) contact layers. Interface roughness is present on the first and third interfaces (from emitter). The no-scattering calculations treat these interfaces in the virtual crystal approximation.[16] We considered three scattering processes: interface roughness (IR), polar optical phonons (POP) and acoustic phonons (AC). IR is modeled as a single layer of alloy where the cations of a single species cluster into islands.[16,22] The exponential correlation length for interface roughness is 6 nm. A screened bulk Hamiltonian is used to model the polar optical phonon interaction.[16,23] A screening length of 50 nm was adopted. Acoustic phonons are considered with the usual assumptions of low energy (elastic) scattering and high temperature.[16,23] Unless specified, all simulations are carried out at 4.2 K to avoid $\Gamma$-$X$-$\Gamma$ tunneling in AlAs barriers. The calculations have been performed using multiple sequential scattering (MSS) theory with six scattering events for elastic scattering and a single sequential scattering for polar optical phonons. It was shown that only a few scattering events are needed in the MSS algorithm to converge with a self-consistent Born calculation.[16] The $I$-$V$ characteristics are presented, for the device shown in Fig. 1, in Fig. 2. The peak current is determined by the alignment of the emitter quasibound state (represented by the bold horizontal line in the emitter side of the device in Fig. 1) and the well state (shown by the bold horizontal line in the well).

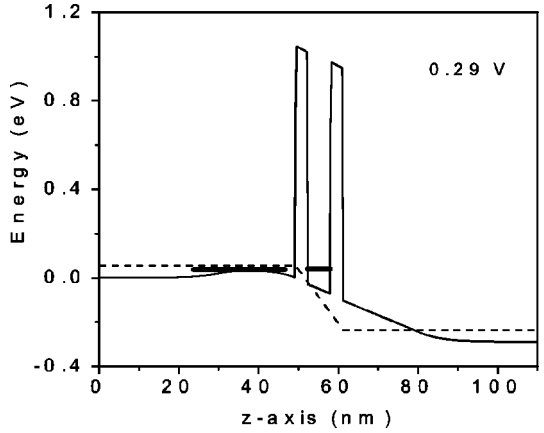


FIG. 1. Band structure of our RTD. The dashed line represents the Fermi level. The horizontal bold straight segments represent the quantized levels in the emitter (left) and central well (right). The bias voltage is 0.29 V.

The dominant scattering process is due to the interface roughness, while the influence of acoustic phonons is negligibly small at this temperature. In numerical calculations[24] we integrate first over the transverse momentum and then we plot the current density as a function of the length of the device in units of nm and other energy coordinates [total energy ($E_t$) or longitudinal energy ($E_z$), respectively, in units of eV]. For convenience we denote by $J_{Et}$ the graph of current density as a function of length of the device and total energy, and by $J_{Ez}$ the graph of current density as a function of length of the device and longitudinal energy.

(*a*) *Coherent Transport.* $J_{Et}$ and $J_{Ez}$ for coherent transport (no scattering) are shown in Fig. 3 at the bias voltage of 0.27 V on linear scale. $J_{Ez}$ is sharply spiked at the resonance energy and needs to be resolved well on a linear or logarithmic scale.[24] The resonance energy is close to 44 meV [Figs. 3(b) and 3(d)]. The homogeneity manifested by $J_{Ez}$ along the device just proves the Tsu-Esaki formulation of coherent transport. In addition, the flat shape of $J_{Et}$ along $E_t$ shows that, at low temperatures, the current is similar for all transverse momenta, with the total energy ranging from resonance energy (which is along the $z$ direction) to the Fermi level, which is at 54.4 meV.

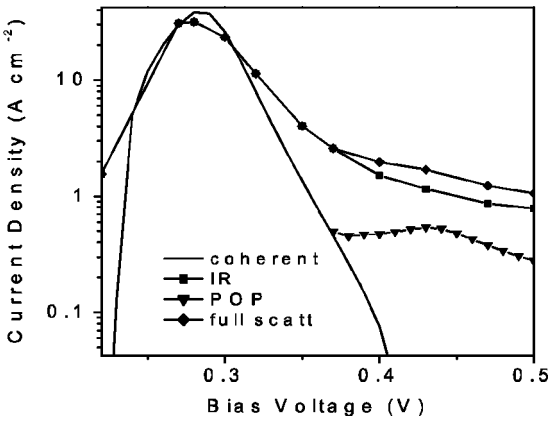


FIG. 2. *I-V* curves. The solid line is for coherent scattering. The solid line with the symbol (□) is for IR scattering, the solid line with the symbol (△) is for POP scattering, and the solid line with the symbol (◇) is for all scattering mechanisms turned on (IR, POP, and AC). One can see the phonon echo as a shoulder on the POP curve.

(*b*) *Off-center current flow at on-resonance bias.* Effects of scattering on $J_{Et}$ and $J_{Ez}$ are shown at two bias points: peak current at 0.27 V (Fig. 4) and valley current at 0.37 V (Fig. 5). With the discussion at these bias points we will show that there is significant off-center current flow on and off resonance. Cross-sections are plotted underneath their corresponding 3D graphs to show the changes occured along $z$ axis.[24] The variation of $J_{Ez}$ along the device signifies a breakdown of the Tsu-Esaki formula in the case of scattering assisted tunneling. Scattering self-energies shift down and broaden the peak of $J_{Ez}$ from its coherent position. When all three scattering mechanisms are turned on, the most striking effect in $J_{Ez}$ is observable at the interfaces, where the roughness scattering is acting. The largest difference in $J_{Ez}$ occurs at the end of the simulated device region. This can be better seen by plotting the cross-section of $J_{Ez}$ shown in Figs. 4(c), 4(d) and 4(g). Once the carriers reached the point $z=50$ nm, $J_{Ez}$ becomes broader, shifted to the left (lower energy) and with some small peak at the energy of 37 meV.[24] At $z=60$ nm in the device $J_{Ez}$ preserves some characteristics of the coherent transport. A similar behavior is also observed just for the interface roughness scattering. This similarity simply suggests that IR scattering is the major effect near the current peak. Disregarding the $z$ variation of $J_{Ez}$ the shifting and broadening are included in phenomenological theory.[20] However, at the voltage 0.27 V, the small peak at $E_z=37$ meV comes from interface roughness scattering, and it can be better seen on $J_{Et}$ (on both the 3D plot and in cross section), where it shows up as a high and sharp peak.

At the bias of 0.27 V in contrast to coherent transport, where $J_{Et}$ is flat (no peaks), the main peak of $J_{Et}$ is at energies close to the Fermi level [also see Figs. 4(f) and 4(h)]. This main peak close to Fermi level leaves 10 meV for transverse energy, which is the difference between the total energy at the main peak in $J_{Et}$ and the resonance (longitudinal) energy along the $z$ axis needed for electrons to tunnel. This difference in energy between the main peak in $J_{Et}$ and the resonance energy along the $z$ axis is a clear proof for off-center flow of electrons in RTD's and it is the central result of our work. The off-center flow is induced by the dominant IR scattering.

(*c*) *Comparison with prediction of others.* The above results are in agreement with the focusing effect predicted by Fertig, He, and Das Sarma.[25] Fertig *et al.*[25] determined first order and second order corrections to the main coherent peak and they found focusing effects of electrons by impurity scattering, i.e., for the energy of incoming electrons $E>E_{z0}$, with $E_{z0}$ the coherent resonance energy, the transmission probability is peaked for final states whose energy of motion perpendicular to the well matches $E_{z0}$. Our numerical calculations plotted in Figs. 4(a), 4(c), 4(e), and 4(g) show that electrons are ''regrouping'' after IR scattering. The ''regrouping'' is made in the context of resonant tunneling and is counterintuitive because, after scattering, carriers are

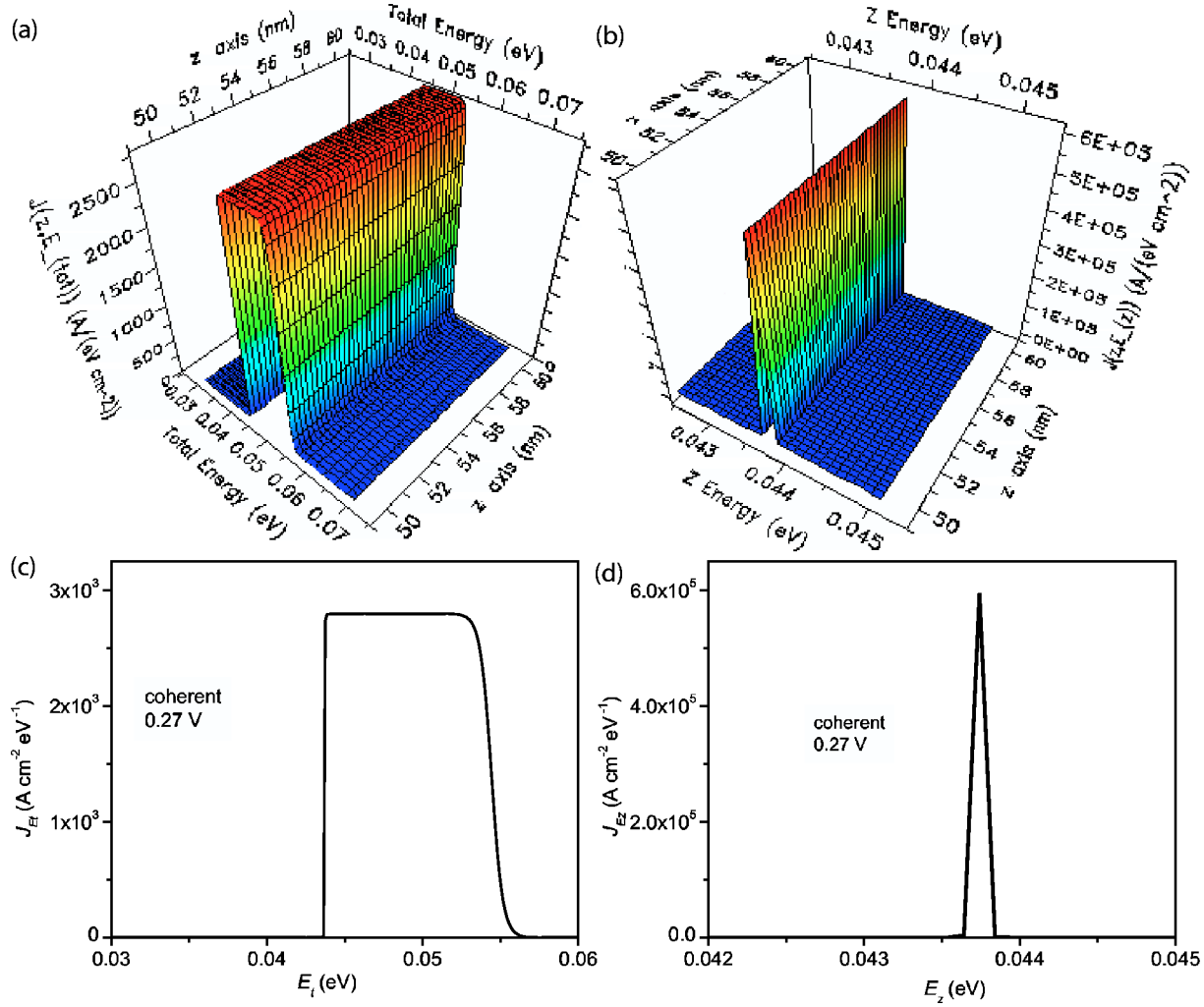


FIG. 3. (Color online) Current density for coherent transport at 0.27 V: (a) $J_{Et}$, (b) $J_{Ez}$, (c) cross section of $J_{Et}$, and (d) cross-section of $J_{Ez}$. The homogeneity of $J_{Ez}$ along the $z$ direction represents the assumptions of the Tsu-Esaki formula.

spread out. In physical terms this behavior is interpreted as follows: because of the scattering, electrons with a wider spread in momentum are forced in the resonance; once electrons pass the scattering center (short-range potential) they will follow the states that are mainly given by coherent transport. In other words, before scattering electrons behave mainly according to a phenomenological prescription,[20] and after the IR scattering electrons regroup according to Fertig *et al.*[25] In addition, the present results show that due to IR scattering electrons are more likely to travel at an angle (oblique) when they cross the RTD.

(*d*) *Off-center current flow at an off-resonance bias.* Dominant off-center current can be observed at the off-resonant bias condition as well (Fig. 5). There is a second peak in $J_{Ez}$ around $E_z = 37$ meV [Figs. 5(a)–5(e) and 5(g)]. This peak is due to the injection from the quasibound state formed in the emitter. At $z = 50$ nm the peak increases significantly. At $z = 60$ nm, the peak is almost the same as the one corresponding to coherent transport. This can be interpreted in the following way. Electrons with $E_z$ around 40 meV (an emitter quasibound state) will be scattered in the well state with $E_z = 10$–$20$ meV [Figs. 5(c), 5(d), and 5(f)]. Thus, electrons will be injected from emitter with $E_z \sim 40$ meV and they will end up with an energy $E_z \sim 16$ meV. The small peak in $J_{Et}$ at $E_z \sim 50$ meV is related to the POP scattering [Figs. 5(f) and 5(h)]. The peak corresponds to the phonon emission and electron scattering to states represented by the sharp features in $J_{Ez}$ around $\sim 16$ meV. Now the difference between on- and off-resonance becomes apparent. In the off-resonance case, scattering will remove resonantly electrons from initial states to final states, and therefore electrons are transferred resonantly from the emitter to the well. The process by itself contributes to the off-zone center current flow since the main scattering is due to interface roughness, which is an elastic process. Also, as expected, it will increase the valley current with respect to coherent transport.

(*e*) *Relative importance of IR versus POP scattering.* At 0.27 V, the effect of polar optical phonons is minimal. The effect of polar optical phonon scattering alone is shown in Figs. 4(b), 4(d), 4(e), and 4(g), and 5(b), 5(d), 5(e), and 5(g). There is a renormalization of resonance energy due to polaronic effects [Figs. 4(d) and 5(d)].[21] The peak in $J_{Ez}$ that

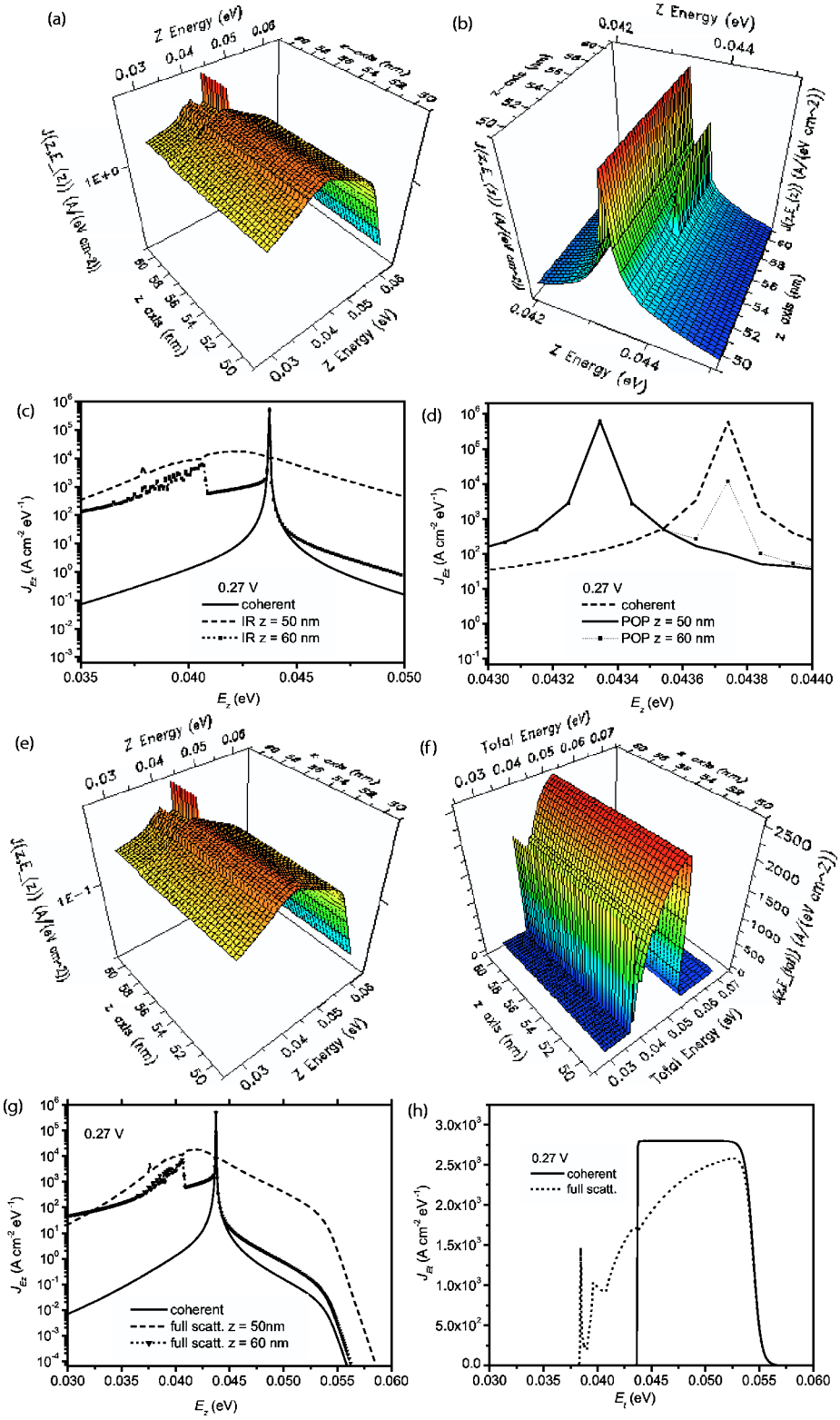


FIG. 4. (Color online) Current density in the presence of scattering at 0.27 V: (a) $J_{Ez}$ for IR scattering; (b) $J_{Ez}$ for POP scattering; (c) cross section of $J_{Ez}$ for IR scattering; (d) cross section of $J_{Ez}$ for POP scattering; (e) $J_{Ez}$ for AC, POP, and IR scattering (AC scattering is negligible); (f) $J_{Et}$ for AC, POP, and IR; (g) cross section of $J_{Ez}$ for AC, POP, and IR scattering; (h) cross-section of $J_{Et}$ for AC, POP, and IR scattering.

dies away in the well corresponds to coherent resonance energy. We may interpret this as electrons which have not interacted with polar optical phonons. The electron state in the well ''dressed'' by POP field contains a cloud of phonons, i.e., a mixture of phonon states.[21,26] The mixture creates fluctuations in the system. Whenever tunneling out into the collector, an electron has one or two phonons, around it, etc.; sometimes the electron has none.[26]

In contrast with interface roughness, a strong effect of polar optical phonon mechanism is felt in the valley region [Figs. 2, 5(f) and 5(h)]. The little spike in $J_{Et}$ before the Fermi level is due to POP scattering [Fig. 5(h)]. At the voltage of 0.37 V the well energy is almost 17 meV. The polaron correction to that energy decreases the energy to about 15.5

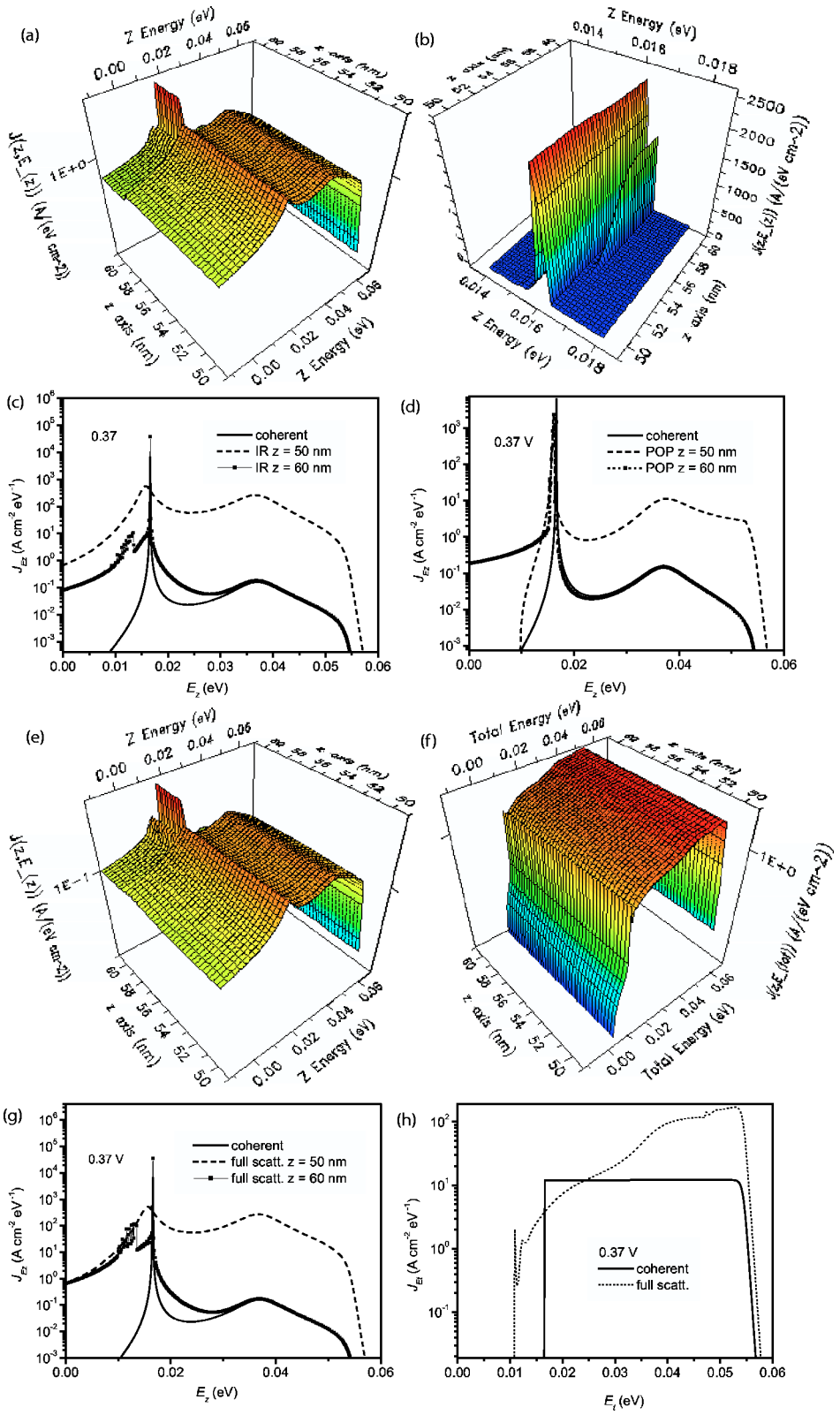


FIG. 5. (Color online) Current density in the presence of scattering at 0.37 V: (a) $J_{Ez}$ for IR scattering; (b) $J_{Ez}$ for POP scattering; (c) cross section of $J_{Ez}$ for IR scattering; (d) cross section of $J_{Ez}$ for POP scattering; (e) $J_{Ez}$ for AC, POP and IR scattering (AC scattering is negligible); (f) $J_{Et}$ for AC, POP, and IR; (g) cross section of $J_{Ez}$ for AC, POP, and IR scattering; (f) cross section of $J_{Et}$ for AC, POP and IR scattering.

meV. By emission of a polar optical phonon with an energy of 36.4 meV, the electrons close to the Fermi energy tunnel resonantly through the device (the energy of POP in GaAs at $\boldsymbol{k}=0$ is 36.4 meV). Thus the on-set bias for polar optical phonons is around 0.37 V.

(*f*) *Off-center current flow induced by AC scattering.* To see the effect of acoustic phonon scattering we increase the lattice temperature at 300 K (Fig. 6). While there is a change in $J_{Ez}$ at 0.27 V [Figs. 6(a) and 6(c)], no change is encountered in $J_{Et}$ compared to the coherent transport. However, the change in both $J_{Ez}$ and $J_{Et}$ is observed at 0.37 V [Figs. 6(b), 6(d), 6(e), and 6(f)]. The change in $J_{Ez}$ as carriers travel

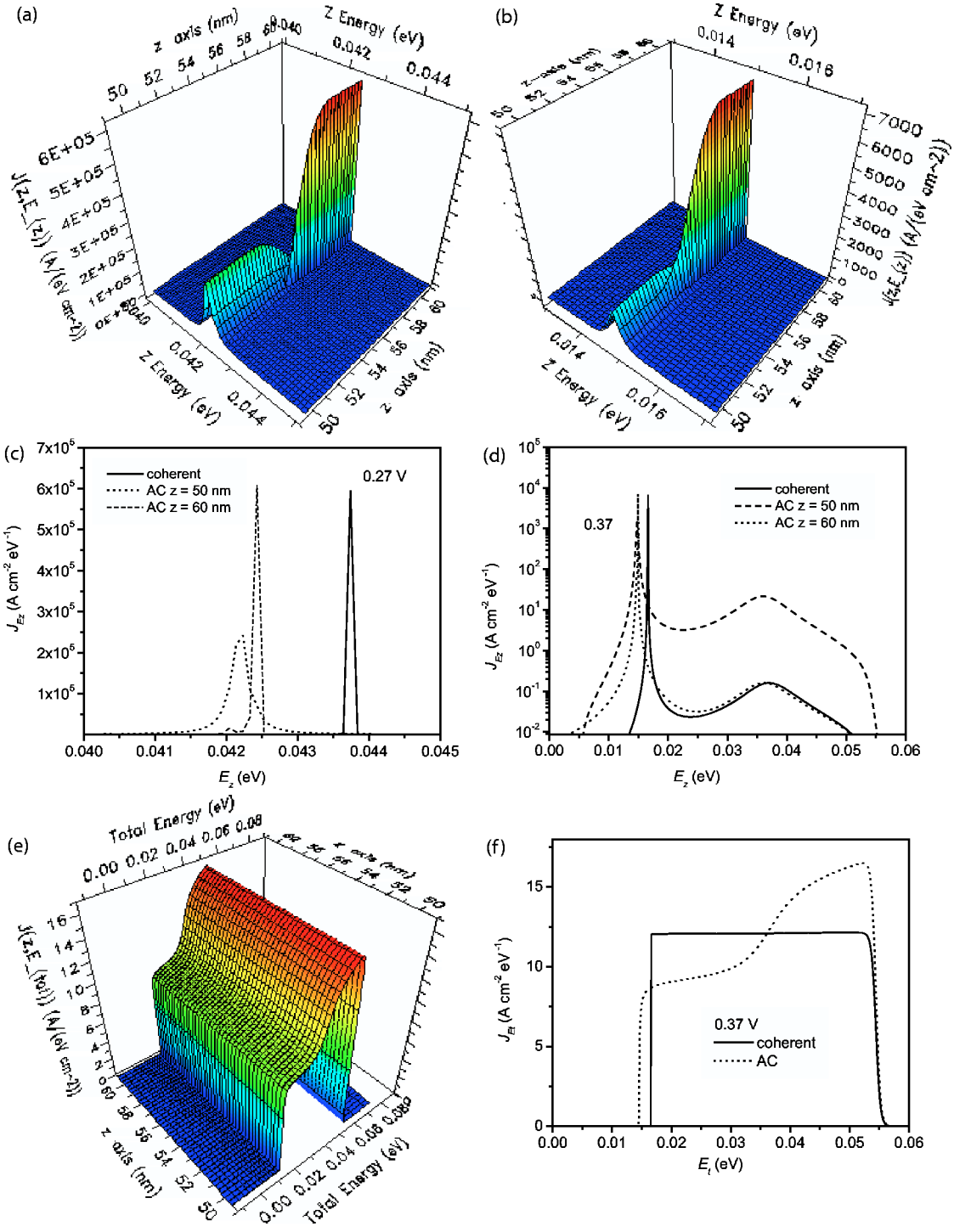


FIG. 6. (Color online) Current density in the presence of AC scattering: (a) $J_{Ez}$ at 0.27 V; (b) $J_{Ez}$ at 0.37 V; (c) cross section of $J_{Ez}$ at 0.27 V (d) cross section of $J_{Ez}$ at 0.37 V; (e) $J_{Et}$ at 0.37 V; (f) cross section of $J_{Et}$ at 0.37 V. The lattice temperature is $T=300$ K.

through the well shows not only the deviation from the Tsu-Esaki formula but also that the scattering is much stronger in the well than in the barriers. A peak in $J_{Et}$ near Fermi level can be seen at this bias [better seen in cross section shown in Fig. 6(f)]. The same analysis carried out previously concludes that the AC mechanism also induces focusing of current flow through a RTD.

## IV. CONCLUSIONS

In summary, we studied the energy dependence of scattering assisted tunnel current in an electron based RTD by using a nonequilibrium Green function approach. Interface roughness, polar optical phonon, and acoustic phonon scatterings are considered. Scattering is associated with the departing from the conventional picture produced by Tsu-Esaki formal-

ism. The current flow is shown to be off center over a large voltage region induced by various scattering mechanisms. Carriers are redirected into the central resonance energy path by an adjustment of their transverse momentum. The Tsu-Esaki type treatment therefore breaks down fundamentally as scattering is introduced into the model.

Interface roughness scattering, which is dominant in the vicinity of the current peak, induces an off-center-current flow across the device. In the presence of resonant tunneling, interface roughness scattering forces electrons with a broader energy dispersion along the $z$ axis to scatter into states with a $z$-axis energy given by the coherent (unperturbed) resonance energy $E_{z0}$.

Phonon scattering becomes effective in the valley region. In the valley region (off resonance), an additional effect occurs for all three mechanisms: the removal of carrier from emitter states into well states, which also contributes to the off-center flow. Moreover, an oblique current flow is also induced by acoustic phonons at high temperature.

This paper is focused on the analysis and mechanisms of off-zone-center current flow. To simplify that analysis we omitted detailed modeling issues such as charge self-consistency and the treatment of large extended contacts. NEMO is perfectly capable of performing such simulations, resulting in a quantitative comparison to experiments as demonstrated in the past.[27–29] We believe that the mechanisms and the off-zone center current flow described in this paper are present in previous NEMO simulations, which focused on the identification of relevant scattering mechanisms and match to experimental data.

## ACKNOWLEDGMENTS

The work described was carried out in part at the Jet Propulsion Laboratory, California Institute of Technology under a contract with National Aeronautics and Space Administration. Funding was provided to JPL by grants from ONR, ARDA, and JPL.

*Electronic address: tsandu@asu.edu. Also at Chemical and Materials Engineering, University of Arizona,Tempe, AZ, 85287-6006.
†URL: http://www-hpc.jpl.nasa.gov/PEP/gekco

[1] J.P.A. van der Wagt, A. Seabaugh, and E.A. Beam III, IEEE Electron. Device Lett. **19**, 7 (1998).
[2] T.P.E. Broekaert, B. Brar, J.P.A. van der Wagt, A.C. Seabaugh, F.J. Morris, T.S. Moise, E.A. Beam III, and G.A. Frazier, IEEE J. Solid-State Circuits **33**, 1342 (1998).
[3] G. Klimeck, R.K. Lake, R.C. Bowen, C.L. Fernando, and W.R. Frensley, VLSI Design **6**, 107 (1998).
[4] R. Tsu and L. Esaki, Appl. Phys. Lett. **22**, 562 (1973).
[5] G. Klimeck, R.C. Bowen, and T.B. Boykin, Superlattices Microstruct. **29**, 187 (2001).
[6] T.B. Boykin, R.E. Carnahan, and K.P. Martin, Phys. Rev. B **51**, 2273 (1995).
[7] T.B. Boykin, Phys. Rev. B **51**, 4289 (1995).
[8] T.B. Boykin, J. Appl. Phys. **87**, 6818 (1995).
[9] R.C. Bowen, G. Kimeck, R. Lake, W.R. Frensley, and T. Moise, J. Appl. Phys. **81**, 3207 (1997).
[10] M.S. Kiledjian, J.N. Schulman, K.L. Wang, and K.V. Rousseau, Surf. Sci. **267**, 205 (1992).
[11] G. Klimeck, R.C. Bowen, and T.B. Boykin, Phys. Rev. B **63**, 195310 (2001).
[12] Y.C. Chung, T. Reker, A.R. Glanfield, P.C. Klipstein, and R. Grey, Phys. Rev. Lett. **88**, 126802 (2002).
[13] G. Klimeck, Phys. Status Solidi B **226**, 9 (2001).
[14] J.N. Schulman, Appl. Phys. Lett. **72**, 2829 (1998).
[15] S. Datta, *Electronic Transport in Mesoscopic Systems* (Cambridge University Press, Cambridge, U.K., 1995).
[16] R. Lake, G. Klimeck, and R.B.D. Jovanovic, J. Appl. Phys. **81**, 7845 (1997).
[17] J. Bardeen, Phys. Rev. Lett. **6**, 57 (1961).
[18] R.K. Lake, G. Klimeck, and S. Datta, Phys. Rev. B **47**, 6427 (1993).
[19] Y. Meir and N.S. Wingreen, Phys. Rev. Lett. **68**, 2512 (1992).
[20] A.D. Stone and P. Lee, Phys. Rev. Lett. **54**, 1196 (1985).
[21] J. Callaway, *Quantum Theory of the Solid State*, 2nd ed. (Academic, New York, 1991).
[22] G. Klimeck, R. Lake, and D.K. Blanks, Phys. Rev. B **58**, 7279 (1998).
[23] B.K. Ridley, *Quantum Processes in Semiconductors*, 3rd ed. (Clarendon, Oxford, 1993).
[24] The $J_{Ez}(E_z,z)$ plots are generated in NEMO for visualization purposes only. In the NEMO code resonances are resolved very well as a function of $E_z$ for every different total energy $E_t$ in the energy range $[-E_0,E_t]$, where $E_0$ is the bottom of the energy range considered in the single band model. The double integral over $E_t$ and $E_z$ is performed in a two-step process with $E_t$ in the outer loop, since the total energies are decoupled (see Ref. 16). For visualization purposes only NEMO can reverse the integration order and generate the $J_{Ez}$ current kernel by integration over $E_t$ first. The actual resolution in $E_z$ of the $J_{Ez}$ plots is determined by the total energy grid and not fine enough to perform a detailed analysis.
[25] H.A. Fertig, S. He, and S.D. Sarma, Phys. Rev. B **41**, 3596 (1990).
[26] G.D. Mahan, *Many-Particle Physics*, 3rd ed. (Kluwer Academic/Plenum, New York, 2000).
[27] G. Klimeck, R. Lake, D. Blanks, C.L. Fernando, R.C. Bowen, T. Moise, and Y.C. Kao, Phys. Status Solidi B **204**, 408 (1997).
[28] R.K. Lake, G. Klimeck, R.C. Bowen, C.L. Fernando, M. Leng, T. Moise, and Y.C. Kao, Superlattices Microstruct. **20**, 279 (1996).
[29] G. Klimeck, R. Lake, C.L. Fernando, R.C. Bowen, D. Blanks, M. Leng, T. Moise, Y.C. Kao, and W.R. Frensley, in *Quantum Devices and Circuits*, edited by K. Ismail, S. Bandyopadhyay, and J.P. Leburton (Imperial, London, 1996).